

NJC

Accepted Manuscript



This is an *Accepted Manuscript*, which has been through the Royal Society of Chemistry peer review process and has been accepted for publication.

Accepted Manuscripts are published online shortly after acceptance, before technical editing, formatting and proof reading. Using this free service, authors can make their results available to the community, in citable form, before we publish the edited article. We will replace this *Accepted Manuscript* with the edited and formatted *Advance Article* as soon as it is available.

You can find more information about *Accepted Manuscripts* in the [Information for Authors](#).

Please note that technical editing may introduce minor changes to the text and/or graphics, which may alter content. The journal's standard [Terms & Conditions](#) and the [Ethical guidelines](#) still apply. In no event shall the Royal Society of Chemistry be held responsible for any errors or omissions in this *Accepted Manuscript* or any consequences arising from the use of any information it contains.



Journal Name

ARTICLE

Au/TiO₂ photocatalysts prepared by solid grinding for artificial solar-light water splitting

Received 00th January 20xx,
Accepted 00th January 20xx

DOI: 10.1039/x0xx00000x

www.rsc.org/

Clément Marchal, Matthieu Behr, Fabrice Vigneron, Valérie Caps, Valérie Keller*

ICPEES, Institute of Chemistry and Processes for Energy, Environment and Health, UMR 7515
CNRS/University of Strasbourg, 25 rue Becquerel, 67087 Strasbourg cedex, France

Here we show in an innovative way that solid grinding is a simple and alternative method for the preparation of solar-light active Au/TiO₂ photocatalysts. We use, for the first time in the solid grinding method, triphenylphosphine gold (I) chloride (AuPPh₃Cl), which has recently been used in solution-based gold catalysts preparation, and chloroauric acid (HAuCl₄), instead of dimethyl gold (III) acetylacetonate [Me₂Au(acac)] as gold precursor. Both compounds yield Au/TiO₂ nanocomposites with interesting activity for artificial solar-light water splitting. In this paper we establish that solid grinding approach to elaborate Au/TiO₂ photocatalyst led to better photocatalytic activity toward artificial solar light water splitting than using chemical reduction method. Effects of the gold loading, of the gold precursor and of the calcination temperature on the photocatalytic activity are described and discussed. The impact of calcination temperature has been highlighted; calcination at 400°C has been found to be the optimal temperature leading to a strong interaction and intimate contact between Au and TiO₂ nanoparticles, thus allowing beneficial electronic effects and stabilization of Au nanoparticles.

Introduction

Sustainable hydrogen production systems are of great importance for the future. Nowadays, more than 90% of the present hydrogen needs are covered by steam reforming of methane, a non-renewable source. Photocatalysis, with its potential to use sunlight for generating hydrogen, represents one of the promising technologies for clean and environmentally friendly hydrogen production and provides a way to use sunlight for generating hydrogen as a renewable green fuel. Since the discovery of photocatalytic water splitting on semi-conductor catalysts by Fujishima and Honda,¹ much effort has been put in the development of photocatalysts that are able to harvest solar energy and to convert it into chemical energy. More precisely, a lot of studies are dealing with TiO₂-based photocatalysts with improved efficiency toward water splitting under solar light illumination.²⁻⁶ The improvement of its photocatalytic water splitting performance can be achieved by many strategies. Amongst them, we can find cationic,^{7,8} anionic⁹⁻¹¹ or co-doping¹²⁻¹⁴ approaches to narrow the band gap energy, addition of electron donors (hole scavengers),^{15,16} and establishment of heterojunctions between TiO₂ and a lower band gap semiconductor¹⁷⁻¹⁹ in order both to photosensitize into visible light and to reduce the charge carriers recombination. Moreover, several research works have reported that the deposition/loading of a precious noble metal, such as Pt, Au, Pd, Rh on a semiconductor surface is beneficial for greatly enhance the

efficiency of photocatalytic water splitting reaction.²⁰⁻²³ The impact of the presence of a noble metal co-catalyst depends on many factors such as the nature of the metal, its content as well as the way of deposition. The enhancement of the photocatalytic activity has also been attributed to the formation of a Schottky barrier at the metal/semi-conductor interface, which leads to electron trapping and efficient charge separation.²⁴ Bamwenda et al.²⁰ compared hydrogen production from water-ethanol solution using different kinds of Au-loaded TiO₂. Different metal particle deposition methods, such as deposition-precipitation, impregnation and photodeposition were also tested. It was found that Au loading prepared by photodeposition worked better than prepared by deposition-precipitation and impregnation. The variations might be explained by the better contact with TiO₂ active sites for photodeposition method. The photocatalytic activity for water splitting on Au-loaded TiO₂ seems to be sensitive to the preparation method. Furthermore, too much metal particle deposition might reduce photon absorption by TiO₂ and might also become electron-hole recombination centers, resulting in lower efficiency. Solid grinding (SG) is a solventless catalyst preparation method. It has proven a quite useful alternative to wet chemistry processes for the preparation of a variety of metal,²⁵⁻²⁸ alloy²⁹ and mixed oxide³⁰ catalysts. In the case of supported metal catalysts, SG consists in manually grinding and mixing for a short time, typically a few minutes, a metal precursor with the powder support, using a mortar and pestle. The operation is carried out at room temperature. Despite the simplicity of the method, the metal precursor is successfully dispersed, at the molecular scale, over the

* e-mail: vkeller@unistra.fr

support. After reduction, often achieved by thermal treatments, supported metal nanoparticles are obtained. All the metal initially introduced as metal complex (or metal salt) is incorporated in the final catalyst, which is of economic significance especially in the case of precious metals such as gold. Besides, despite the absence of solubilization of the metal precursor, high reproducibility is achieved. Hence, this practical method has proven convenient and efficient in producing highly active supported gold catalysts for heterogeneous reactions, such as *e.g.* the epoxidation of propylene,²⁶ the aerobic oxidation of glucose^{27,28} and other alcohols^{2,5}.

In this paper, we carried out as an innovative approach the elaboration of Au/TiO₂ photocatalyst for efficient artificial solar light water splitting using SG preparation method.

Experimental

Materials and syntheses

Titanium (IV) isopropoxide (Ti[OCH(CH₃)₂]₄) (≥ 97%) was purchased from Sigma-Aldrich. Gold (III) chloride hydrate (HAuCl₄) (99.999% trace metals basis) and Chloro-(triphenylphosphine) gold (I) (AuPPh₃Cl) (≥ 99.9% trace metals basis) were also purchased from Sigma-Aldrich. All the chemicals were used without further purification.

Titania (TiO₂) "sol-gel" was obtained via a "low temperature" synthesis. First, an amount of titanium isopropoxide (TIP) precursor was mixed with 40 mL of ethanol at room temperature. To this solution, 40 mL of water (adjusted to pH = 9, by addition of ammonia) was added dropwise. Then, the solution was evaporated under stirring until a dry paste was obtained and dried overnight at 110 °C. To finish, the obtained sample was crushed in an agate mortar and calcined at 400 °C for 3 h (heating rate of 5 °C min⁻¹).

Au/TiO₂ nanocomposites were prepared by solid grinding. Titania (from the sol-gel synthesis, 500 to 1500 mg) and AuPPh₃Cl (unless otherwise mentioned, 1.3 to 13 mg) were mechanically mixed with a pestle in an agate mortar during 10 min at room temperature (about 22 °C). The amount of AuPPh₃Cl was adjusted in order to tune gold loadings from 0.1 wt.% to 1 wt.%. Finally, a calcination step was applied. Calcinations were performed at 200 °C, 400 °C, and 600 °C in order to see the effect of the calcination temperature on the structural and functional properties of the composites. The resulting materials are denoted XAu/TiO₂[Tcal], where X stands for the gold loading in wt.% and Tcal stands for the calcination temperature in °C. Three samples were also prepared with HAuCl₄ (5-13 mg) instead of AuPPh₃Cl as gold precursor. These samples are denoted as XAu[HAuCl₄]/TiO₂[Tcal].

For comparison, two Au/TiO₂ nanocomposites were also prepared by chemical reduction, adapting the procedure described in ref. 31. Titania (500 mg) was dispersed into ethanol with a tip sonicator (25 kHz) during 30 min. A HAuCl₄ solution (C₀=2.5(±0.2)×10⁻³ mol L⁻¹) was added, the volume of which (1.8 mL or 3.1 mL) was adjusted according to the targeted gold loading (0.3 wt. % or 0.5 wt. %). The resulting mixture was left in a bath sonicator (30 W, 35 kHz) for 1 h before 5 mL of a fresh NaBH₄ solution (C₀=2.5×10⁻² mol L⁻¹) was added. The mixture was then sonicated during 2 h. To finish, samples were dried at 110 °C during 12 h. These samples are denoted XAu/TiO₂(CR), where X stands for the theoretical gold

loading in wt.% keeping in mind that a deposition yield of 85% was achieved.

Characterization

X-ray Diffraction (XRD) measurements were carried out on a D8-Advance diffractometer equipped with a LynxEye detector and operated at 40 kV and 40 mA, in a $\theta - 2\theta$ mode using the K _{α 1} radiation of Cu at 1.5406 Å. The datasets are acquired in step-scan mode over the 2 θ range 5 – 90°, using a step interval of 0.041° and a counting time of 94.5s per step. Samples are deposited on a round-shaped glass plate. The datasets are acquired in step-scan mode over the 10-90° 2 θ range. Average size of the titania crystallites is determined using the Scherrer formula from the full width at half-maximum of the TiO₂ (101) reflection at 2 θ = 25.3°.

Thermo-Gravimetric Analysis (TGA) was performed using a TA Instrument Q5000IR. Each sample was placed in a platinum crucible and heated from room temperature to 900 °C with a heating rate of 10 °C min⁻¹ under air flow at 100 cm³ min⁻¹.

Specific surface areas were obtained via the Brunauer, Emmett and Teller (BET) and t-plot methods. The surface area measurements were performed on a Micromeritics Asap 2420 porosimeter using N₂ as an adsorbent at liquid nitrogen temperature. Materials were outgassed at 250 °C for 3 h in order to desorb impurities from their surfaces.

The diffuse-reflectance UV-Visible absorption spectra of composites were recorded on a Cary UV 100 Scan UV/Vis spectrophotometer (Varian).

Photocatalytic study

The photocatalytic activity of the prepared samples was evaluated toward the water-splitting reaction. Hydrogen production was carried out in a Quartz reactor containing 1 L of Milli-Q water and equipped with a plunging quartz tube containing a 150 W CERAMIC-Metal-Halide Lamp (light emission spectra shown in Figure 1) with a low UV-A content and a large part in the visible light range. This artificial light is used in our experimental conditions for simulating solar-light irradiation. The measured irradiance was 30 mW/cm². The photocatalytic tests were performed with 250 mg of catalyst under 100 mL min⁻¹ nitrogen flow with a mechanical stirring at 700 rpm. Prior to any experiment, residual oxygen was removed by nitrogen flushing. Pure water was used as hydrogen source and

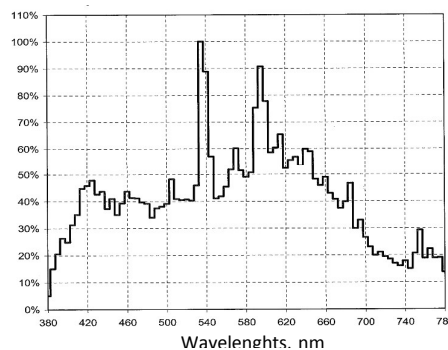


Figure 1: Emission spectrum of the artificial solar light (metal halide 150 W)

methanol was added as sacrificial agent (0.1 to 1% volumetric) to

enhance H_2 production. The reaction products were analyzed on-line every 100 s by thermal conductivity detectors (TCD) on a micro-gas chromatography Gaz Analyser R-3000 SRA Instruments. All experiments were performed under the same conditions.

Results

All Au/TiO₂ nanocomposites used in this study exhibit a purple color indicative of the presence of gold nanoparticles (Au NP) in the samples. For the series of composites prepared by solid grinding, the shade of purple intensifies with increasing gold loading, showing the presence of more gold within the composite.

Influence of the gold loading

Figure 2 shows the influence of the gold loading of Au/TiO₂ [200] nanocomposites on the amount of hydrogen evolved from water splitting as a function of the amount of sacrificial agent. It can be seen that, whatever the amount of methanol present, increasing the gold loading from 0.1 to 0.2 wt.% doubles the activity of the composite. The production of hydrogen is again nearly doubled by further increasing the gold loading to 0.5 wt.%. Nearly 470 μmol of H_2 are produced per hour per gram on the 0.5Au/TiO₂[200] sample in the presence of 10 mL of methanol. Further increasing the loading of gold to 1 wt.%, on the other hand, results in a major decrease of the photocatalytic activity of about 60%. 1Au/TiO₂[200] remains only 50% more active than 0.1Au/TiO₂[200]. This is attributed to enhanced recombination of the charges produced by the semi-conductor at the possibly more numerous metal nanoparticles/TiO₂ interface.²² The gold loading comprised between 0.5 and 1 wt.% have not been investigated. Hence, amongst the photocatalytic systems studied here, 0.5 wt.% appears to be the optimal loading of gold for efficiently splitting water and maximizing hydrogen production under our conditions. Similar metal loadings have proven beneficial to enhance the photocatalytic activity of titania in other studies.²²

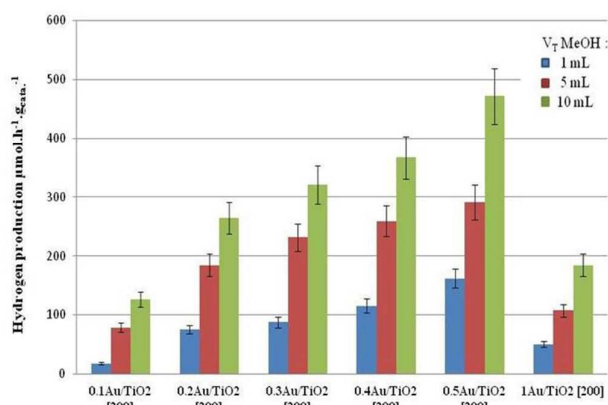


Figure 2: Impact of the gold loading of Au/TiO₂[200] nanocomposites on the amount of hydrogen produced in the water splitting reaction carried out in the presence of 1, 5, or 10 mL of methanol.

The same trend can be observed with the composites prepared with HAuCl₄ (Figure 3): 0.5 wt% Au appears to be the optimal loading, although the difference between 0.3 and 0.5 wt% is less pronounced than for the composites prepared with AuPPh₃Cl

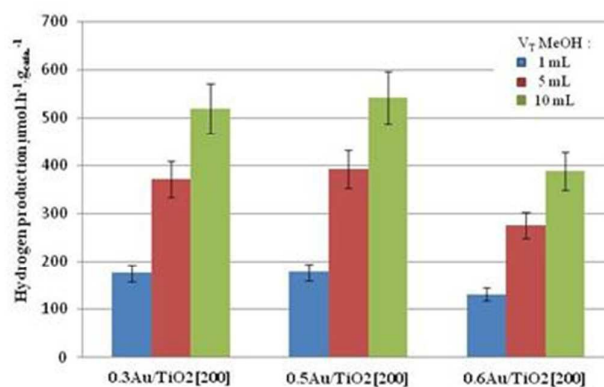


Figure 3: Impact of the gold loading of Au[HAuCl₄]/TiO₂[200] nanocomposites on the amount of hydrogen produced in the water splitting reaction carried out in the presence of 1, 5, or 10 mL of methanol.

(Figure 2). Increasing the gold loading to 0.6 wt.% however leads to a 30% loss of the photocatalytic activity of the Au[HAuCl₄]/TiO₂[200] composite (carrying out the reaction with 10 mL methanol).

Hence, a gold loading of 0.5wt.% seems optimal to boost the photocatalytic activity of titania in water splitting, whatever the gold precursor used in solid grinding. It must be noted that, for a final calcination at 200°C, using HAuCl₄ leads to a slightly higher activity than using AuPPh₃Cl as precursor. Any larger loading of gold markedly reduces the catalytic enhancement.

Influence of the atmosphere of the post-synthesis treatment of HAuCl₄/TiO₂ mechanical mixtures

Using hydrogen instead of air, during thermal treatment of the mechanical mixtures of HAuCl₄ and TiO₂ at 200°C, does not result in any improvement in the photocatalytic activity of the resulting composite (Figure 4). Hydrogen treatment is actually detrimental to the activity: 0.5Au[HAuCl₄]/TiO₂[200] in particular loses up to 30% of its activity if treated under hydrogen instead of air. This effect is slightly less pronounced in the case of 0.3Au[HAuCl₄]/TiO₂[200], but it is still present.

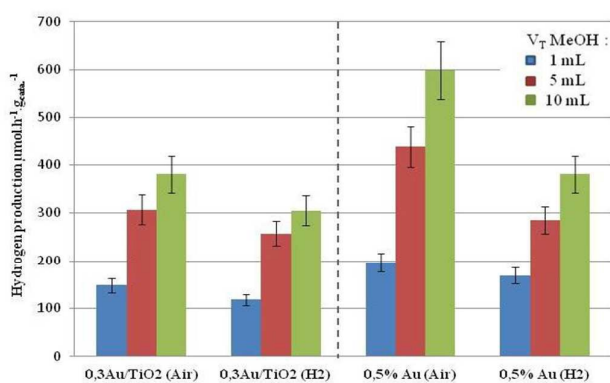


Figure 4: Impact of the atmosphere of the thermal treatment of Au[HAuCl₄]/TiO₂[200] nanocomposites on the amount of hydrogen produced in the water splitting reaction carried out in the presence of 1, 5 and 10 mL of methanol.

Influence of the calcination temperature of AuPPh₃Cl/TiO₂ mechanical mixtures

Figure 5 shows the influence of the calcination temperature of Au/TiO₂ nanocomposites on the amount of hydrogen evolved from water splitting. Only the most effective composites, in term of gold utilization, are presented. Besides, only the results obtained in the presence of 10 mL methanol, which allows to get the highest hydrogen productions under our conditions, are shown. It appears that, whatever the gold loading of the composite, calcining the mechanical mixtures of AuPPh₃Cl and TiO₂ at 400 °C yields the largest amounts of hydrogen, as compared with the calcinations performed at 200 °C and 600 °C. It is also interesting to mention that whatever the calcination temperature, 0.5Au/TiO₂ remains the most active composite. Its activity of about 470 μmol H₂ h⁻¹ g_{cata}⁻¹ can be boosted by about 25% by increasing the calcination temperature from 200 to 400 °C. 0.5Au/TiO₂[400] thus yields 590 μmol H₂ h⁻¹ g_{cata}⁻¹. It surpasses the composites prepared from mechanical mixtures of HAuCl₄ and TiO₂ (Figure 3).

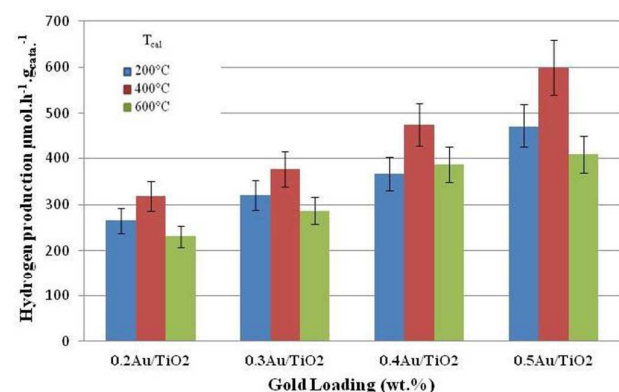


Figure 5: Impact of the calcination temperature of Au/TiO₂ nanocomposites on the amount of hydrogen produced in the water splitting reaction carried out in the presence of 10 mL of methanol.

In summary, 0.5Au/TiO₂[400] is the best composite of the study, in terms of photocatalytic hydrogen production from water splitting. Its activity reaches 590 μmol H₂ h⁻¹ g_{cata}⁻¹ in the presence of 10 mL of methanol. In the next section, we will present the structural parameters leading to such photocatalytic performance, which will allow us to hypothesize on the reasons for the optimal efficiency of calcining AuPPh₃Cl/TiO₂ mechanical mixtures at 400 °C.

Discussion

Effect of calcination on the physico-chemical properties of Au/TiO₂

Samples	S _{BET} (m ² g ⁻¹)	Crystallite size (nm)	
		Anatase	Rutile
TiO ₂ "solgel"	117	18.1	/
0.5Au/TiO ₂ [200]	140	17.9	/
0.5Au/TiO ₂ [400]	121	17.2	/
0.5Au/TiO ₂ [600]	38	24.5	45

Table 1: Physico-chemical properties of 0.5Au/TiO₂, including surfaces areas (S_{BET}) and titania crystallite sizes, as derived from XRD using the Debye-Scherrer formula.

After grinding the TiO₂ "solgel" material with AuPPh₃Cl and calcining the mixture at 200 °C, an increase in the surface area (from 117 to 140 m²g⁻¹) is observed (Table 1). This was rather unexpected since titania was already calcined at 400 °C prior to its introduction in the grinding mixture. The action of mechanical grinding at room temperature, followed by calcination at a mild temperature, is unlikely to reduce the intrinsic size of the anatase crystallites. This is indeed confirmed by calculation of the average size of the titania crystallites as derived from XRD spectra (Figure 6), using the Debye-Scherrer formula on the intense TiO₂ (101) reflection: the size of the anatase crystallites contained in the starting TiO₂ "solgel" is unchanged upon solid grinding with AuPPh₃Cl and calcination at 200 °C. To account for the non-negligible increase in surface area, we must thus assume that 0.5Au/TiO₂[200] contains a certain amount of organics, which must have been introduced upon mixing with AuPPh₃Cl. It implies that calcination at 200 °C does not lead to the complete reduction of gold and that ligands (or products of their decomposition) still persist in 0.5Au/TiO₂[200], as will be evidenced and discussed below, in the TGA section. After calcination at 400 °C, the composite retrieves the surface area of the starting TiO₂ "solgel" and the average anatase crystallite size remains unchanged. Hence, it can be concluded that calcination at 400 °C only mildly affects the structural and morphological properties of the composite. However, calcination at 600 °C causes a drastic decrease in surface area (from 121 to 38 m²g⁻¹), associated with an increase in the average size of the anatase crystallites, which is typical of the behavior of oxides.³²⁻³⁴ The increase in crystallite size is however moderate compared to the loss of surface area, which suggests that some aggregation has occurred during the process. The rutile phase has also been formed as evidenced by XRD (Figure 6).

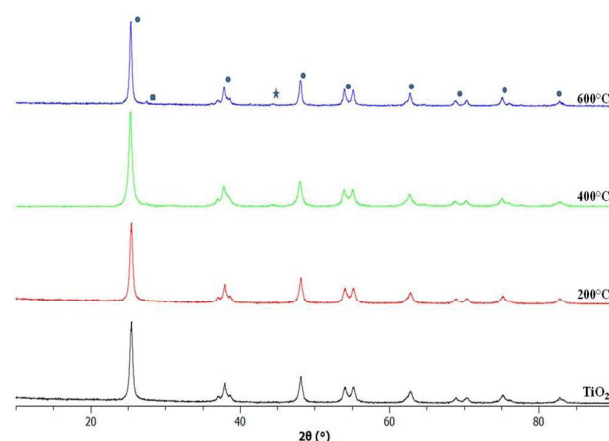


Figure 6: (a) Diffractograms of TiO₂ and 0.5Au/TiO₂ calcined at different temperatures, showing anatase TiO₂ (●), rutile TiO₂ (■) and gold (★) reflections. The diffractogram of the parent TiO₂ "solgel" is shown for comparison.

Concerning the gold component of the composite, the presence of the surface plasmon resonance (SPR) in the absorption spectra of all Au/TiO₂ composites (Figure 7) is a clear indication that gold is present as nanoparticles. While the SPR is positioned at about 550 nm for the composites calcined at 200 °C (Figure 7a), it shifts to about 580 nm when calcination is performed at 400 °C (Figure 7b) and to about 600 nm (Figure 7c) when the calcination is performed at 600 °C. This red-shift (Figure 7d) is typical of an increase in the refractive index of the composite. This is consistent with the

increase in the crystallinity of the titania component of the composite observed by XRD (Figure 6).³⁵ Besides, the intensity of the SPR appears only mildly affected by increasing the calcination temperature from 200 to 400 °C. However, further increasing the calcination temperature to 600 °C results in a clearly more intense SPR band. This suggests that the size of the gold nanoparticles (Au NP) initially present in the Au/TiO₂[200] composites has markedly increased upon calcination at 600 °C. This is generally observed at these temperatures, due to the relatively low melting point of gold (1064 °C) and the resulting low Tammann temperature of Au NP.³⁶ Actually, the low intensity of the SPR band exhibited by the composites calcined at 400 °C, associated with a broad and weak Au (200) reflection in the XRD spectrum (Figure 8), indicates that Au NP are well-stabilized within the composites. Hence, the sintering, which leads to a marked increase in Au NP size and which is often observed at this temperature in Au/TiO₂ catalysts prepared by other methods,^{37,38} has also been evidenced in our case, looking at the TEM particles size distribution (Figure 9).

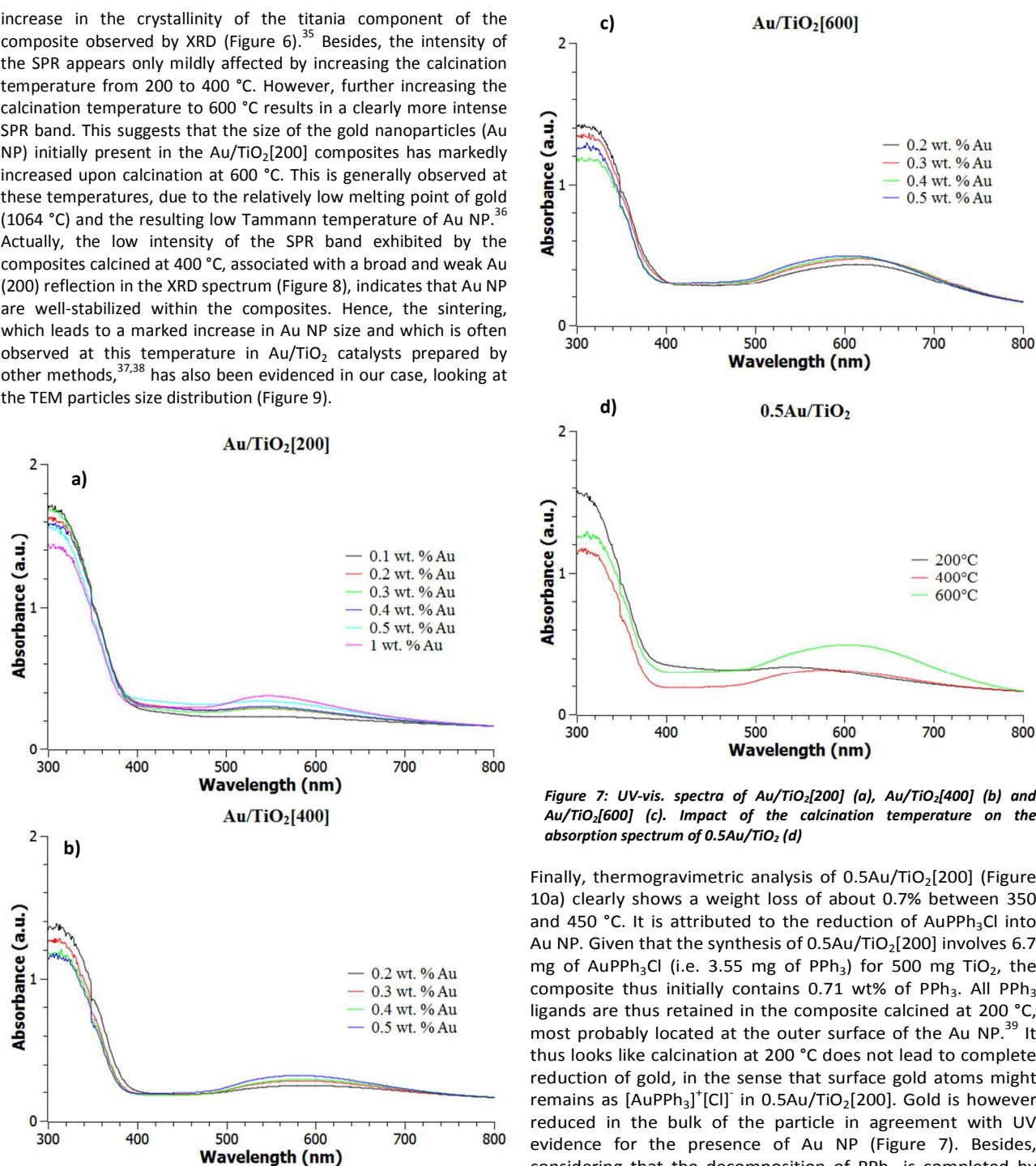


Figure 7: UV-vis. spectra of Au/TiO₂[200] (a), Au/TiO₂[400] (b) and Au/TiO₂[600] (c). Impact of the calcination temperature on the absorption spectrum of 0.5Au/TiO₂ (d)

Finally, thermogravimetric analysis of 0.5Au/TiO₂[200] (Figure 10a) clearly shows a weight loss of about 0.7% between 350 and 450 °C. It is attributed to the reduction of AuPPh₃Cl into Au NP. Given that the synthesis of 0.5Au/TiO₂[200] involves 6.7 mg of AuPPh₃Cl (i.e. 3.55 mg of PPh₃) for 500 mg TiO₂, the composite thus initially contains 0.71 wt% of PPh₃. All PPh₃ ligands are thus retained in the composite calcined at 200 °C, most probably located at the outer surface of the Au NP.³⁹ It thus looks like calcination at 200 °C does not lead to complete reduction of gold, in the sense that surface gold atoms might remain as [AuPPh₃]⁺[Cl]⁻ in 0.5Au/TiO₂[200]. Gold is however reduced in the bulk of the particle in agreement with UV evidence for the presence of Au NP (Figure 7). Besides, considering that the decomposition of PPh₃ is completed by 220 °C in a dynamic calcination process (Figure 10b), and that the decomposition of bulk/free AuPPh₃Cl is completed by 250 °C under such conditions, it seems that AuPPh₃Cl/PPh₃ is stabilized in the composite enough to shift its full decomposition temperature by 200 °C (under dynamic conditions). Hence calcination at 400 °C (maintained for 4 h) is needed in order to fully decompose the gold complex and its ligands.

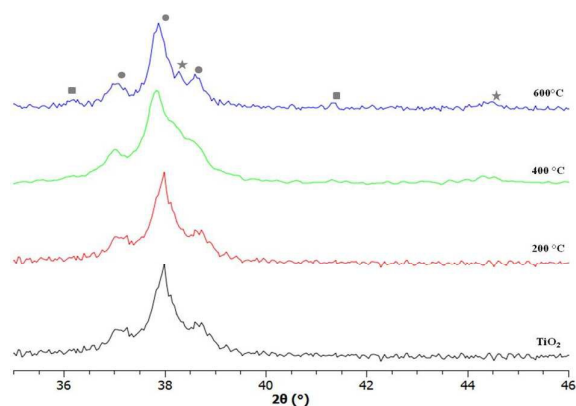


Figure 8: Diffractograms of $0.5\text{Au}/\text{TiO}_2$ calcined at different temperatures, highlighting the Au (111) and Au (200) reflections at 38.2° and 44.5° respectively (★). The diffractogram of the parent TiO_2 “sol-gel” is shown for comparison.

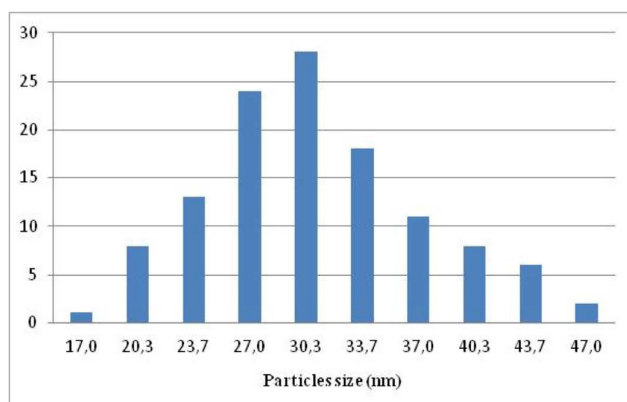


Figure 9: Au mean size particles distribution of $\text{Au}/\text{TiO}_2[600]$ composites

The TGA profile of $0.5\text{Au}/\text{TiO}_2[400]$ (Figure 10a) is subsequently similar to that of TiO_2 (Figure 9c), indicating indeed the absence of $\text{AuPPh}_3\text{Cl}/\text{PPh}_3$ in the material. It seems that full reduction of gold, achieved by calcining the mechanical mixtures of AuPPh_3Cl and TiO_2 at 400°C , allows to maximize the photocatalytic activity of the composite in the water splitting reaction. While PPh_3 residues at the proximity of Au NP are useful for stabilizing Au NP size, their presence proves detrimental to the photocatalytic activity of titania. A negative impact of the presence of PPh_3 residues has also been observed in Au/silica catalysts used for the aerobic epoxidation of stilbene.⁴⁰ In this case, accessibility of part of the catalytic Au surface is clearly blocked. In photocatalytic processes, on the other hand, we speculate that these residues might prevent direct contact between Au NP and titania, thus inhibiting favorable electronic effects for photocatalysis. Direct, strong interaction between Au NP and titania might indeed be key for Au NP to enhance the activity of TiO_2 photocatalysts. We suppose that the intimate contact between Au NP and TiO_2 surface has a strong impact both (i) on the co-catalyst role of Au NP and on (ii) the

efficient role of Au NP as co-catalyst benefits from a better impact both (i) on the co-catalyst role of Au NP and on (ii) the metal/semiconductor interface (Figure

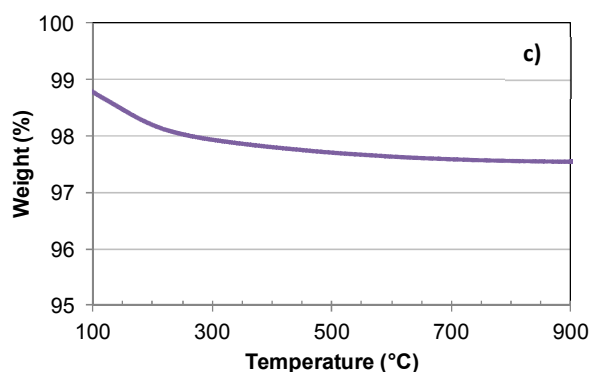
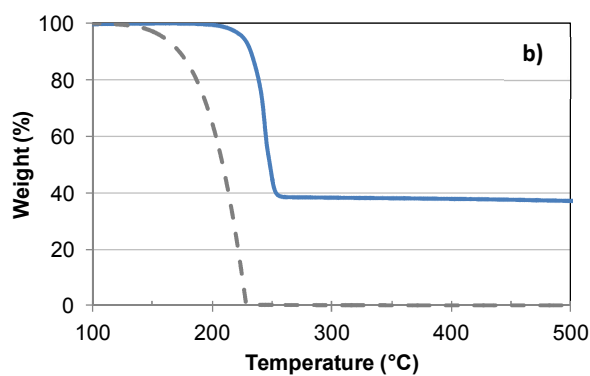
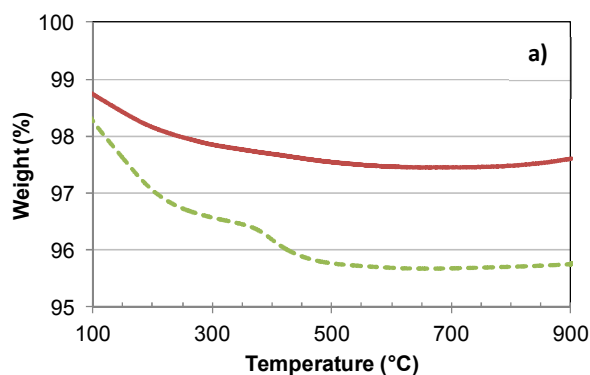


Figure 10: TGA of $0.5\text{Au}/\text{TiO}_2[200]$ (---) and $0.5\text{Au}/\text{TiO}_2[400]$ (a), PPh_3 (---) and AuPPh_3Cl (b) and TiO_2 (from the sol-gel synthesis) (c)

photogenerated electron transfer from activated TiO_2 to Au NP leading to catalytic H^+ reduction into H_2 on the metal NP. The enhancement of photocatalytic activity due to close contact of the two components can also be attributed to the formation of a Schottky barrier at the metal/semi-conductor interface, which leads to electron trapping on Au NP and thus efficient charge separation limiting recombination phenomena.

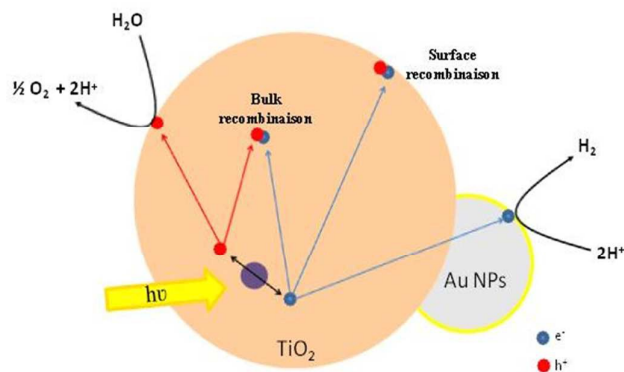
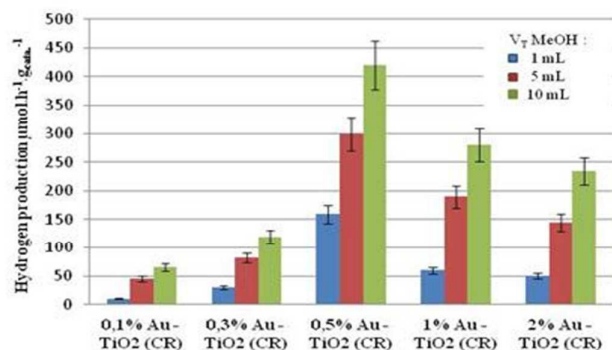


Figure 11: Au/TiO₂ intimate junction. Au NP act as co-catalyst and for enhancing photogenerated charges separation.

Comparison between solid grinding and chemical reduction

The activity of the Au/TiO₂ nanocomposites elaborated via the solid grinding method was compared to that of Au/TiO₂ photocatalysts prepared by chemical reduction method (Figure 12). It must be highlighted that for Au loadings ranging below 0.5 wt.%, chemical reduction led to lower photocatalytic activity towards artificial solar light water splitting. Hydrogen production rates indeed appear at least 40% lower than using the composites prepared by solid grinding, whether starting from AuPPh₃Cl (Figure 2) or using HAuCl₄ (Figure 3). The gold loadings, on the other hand, are only 15% lower than those of the solid grinding samples. Given the effect of the calcination temperature of the photocatalytic activity described previously, the lower activity of the CR samples may come from the



absence of thermal treatment in the CR method.

Figure 12: Impact of the gold loading of Au/TiO₂ (CR) nanocomposites on the amount of hydrogen produced in the water splitting reaction carried out in the presence 1, 5, or 10 mL of methanol.

Conclusion

In this paper we highlighted the interest of solid grinding as simple an innovative approach for the elaboration of Au/TiO₂ photocatalysts for H₂ production by artificial solar light water splitting. We used, for the first time in the solid grinding method, triphenylphosphine gold (I) chloride (AuPPh₃Cl) as Au precursor. Using this precursor, it has been shown that a final calcination step higher than 250°C is required to completely eliminate AuPPh₃Cl

residues. Calcination at 400°C has been found to be the optimal temperature leading to a strong interaction and intimate contact between Au and TiO₂ nanoparticles. This strong interaction helps to beneficial electronic effects. Indeed we suppose that the intimate contact between Au and TiO₂ nanoparticles induces photogenerated electron transfer from TiO₂ to Au NPs yielding enhanced co-catalyst activity and better charges separation. These two positive effects can explain the enhanced photocatalytic activity toward solar light water splitting to produce H₂.

Acknowledgements

The authors acknowledge the Region Alsace for financial support and Dr. Anne Boos (IPHC Strasbourg) for ICP analyses.

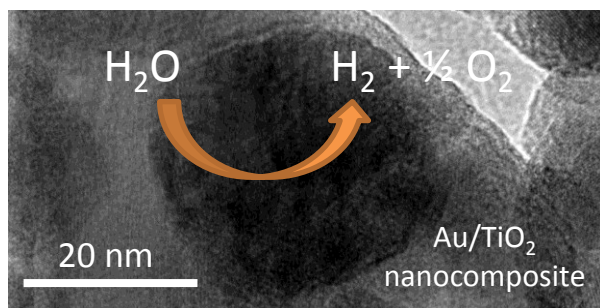
References

1. A. Fujishima and K. Honda, *Nature* 1972, **238**, 37.
2. Z. Zou, J. Ye and K. Sayama, *Nature* 2001, **414**, 625.
3. R. Abe, T. Takata, H. Sugihara and K. Domen, *Chem. Comm.*, 2005, 3829.
4. P. Dhanasekaran and N.M. Gupta, *Int. J. Hydrogen Energy*, 2012, **37**, 4897.
5. K.M. Parida, K.H. Reddy, S. Martha, D.P. Das and N. Biswal, *Int. J. Hydrogen Energy*, 2010, **35**, 12161.
6. M. Ashokkumar, *Int. J. Hydrogen Energy*, 1998, **23**, 427–38.
7. W.Y. Choi, A. Termin and M.R. Hoffmann, *J. Phys. Chem.*, 1994, **84**, 13669.
8. D. Dvoranova, V. Brezova, M. Mazur and M. Malati, *Appl Catal B: Environ*, 2002, **37**, 91.
9. R. Asahi, T. Morikawa, T. Ohwaki, K. Aoki and Y. Taga, *Science*, 2001, **293**, 269.
10. T. Ohno, M. Akiyoshi, T. Umeyayashi, K. Asai, T. Mitsui and M. Matsumura, *Appl Catal A: Gen*, 2004, **265**, 115.
11. M. Ni., M. K.H. Leung, D. Y. C. Leung and K. Sumathy, *Renewable and Sustainable Energy Reviews*, 2007, **11**, 401.
12. R. Long and N.J. English, *Chem. Phys. Lett.*, 2009, **478**.
13. W.-J. Yin, H. Tang, S.-H. Wei, M. M. Al-Jassim, J. Turner and Y. Yan, *Phys. Rev. B* 2010, **82**, 045106.
14. T. Cottineau, N. Béalu, P.-A. Gross, S.N. Pronkin, N. Keller, E.R. Savinova and V. Keller, *J. Mater. Chem.*, 2013, **1**, 2151.
15. A.A. Nada, M.H. Barakat, H.A. Hamed, N.R. Mohamed, T.N. Veziroglu, *Int J Hydrogen Energy*, 2005, **30**, 687.
16. Y.X. Li, G.X. Lu, S.B. Li, *Chemosphere*, 2003, **52**, 843.
17. K. Gurunathan, P. Maruthamuthu and V.C. Sastri, *Int. J. Hydrogen Energy*, 1997, **22** 57.
18. P. Dhanasekaran and N.M. Gupta, *Int. J. Hydrogen Energy*, 2012, **37**, 4897.
19. K.M. Parida, K.H. Reddy, S. Martha, D.P. Das and N. Biswal, *Int. J. Hydrogen Energy* 2010, **35**, 12161.
20. G.R. Bamwenda, S. Tsubota, T. Nakamura and M. Haruta. *J Photochem Photobiol A: Chem* 1995, **89**,177.
21. S. Sakthivel, M.V. Shankar, M. Palanichamy, B. Arabindoo, D.W. Bahnemann and V. Murugesan, *Water Res.*, 2004, **38**, 3001.
22. O. Rosseler, V.S. Muthukonda, M. Karkmaz-Le Du, L. Schmidlin, N. Keller and V. Keller, *J. Catal.*, 2010, **269**, 179.
23. M.C. Blount, J.A. Buchholtz and J.L. Falconer, *J. Catal.*, 2001, **197**, 303.
24. M. Ishida, M. Nagaoka, T. Akita and M. Haruta, *Chem. Eur. J.*, 2008, **14**, 8456.
26. J. Huang, T. Akita, J. Faye, T. Fujitani, T. Takei and M. Haruta, *Angew. Chem. Int. Ed.*, 2009, **48**, 7862.
27. H. Okatsu, N. Kinoshita, T. Akita, T. Ishida and M. Haruta, *Appl.*

ARTICLE

Journal Name

- Catal. A*, 2009, **369**, 8.
28. T. Ishida, H. Watanabe, T. Bebeko, T. Akita and M. Haruta, *Appl. Catal. A*, 2010, **377**, 42.
29. J. Kugai, T. Moriya, S. Seino, T. Nakagawa, Y. Ohkubo, H. Nitani and T. A. Yamamoto, *Catal Lett.*, 2013, **143**, 1182.
30. H. Zhu, D.C. Rosenfeld, D.H. Anjum, V. Caps and J.-M. Basset, *ChemSusChem*, 2015, **8**, 1254.
31. F. Vigneron, A. Piquet, W. Baaziz, P. Ronot, A. Boos, I. Janowska, C. Pham-Huu, C. Petit and V. Caps, *Catal. Today*, 2014, **235**, 90.
32. H. Zhu, S. Ould-Chikh, D. H. Anjum, M. Sun, G. Biauxque, J.-M. Basset and V. Caps, *J. Catal.*, 2012, **285**, 292.
33. P. Laveille, G. Biauxque, H. Zhu, J.-M. Basset and V. Caps, *Catal. Today*, 2013, **203**, 3-9.
34. H. Zhu, H. Dong, P. Laveille, Y. Saih, V. Caps and J.-M. Basset, *Catal. Today*, 2014, **228**, 58.
35. P. Lignier, M. Comotti, F. Schüth, J.-L. Rousset and V. Caps, *Catal. Today*, 2009, **141**, 355 and references therein.
36. V. Caps, *L'Actualité Chimique*, 2010, **337**, 18 and references therein.
37. V. Mendez, V. Caps and S. Daniele, *Chem. Commun.*, 2009, 3116.
38. V. Mendez, K. Guillois, S. Daniele, A. Tuel and V. Caps, *Dalton Trans.*, 2010, **39**, 8457.
39. Y. Liu, H. Tsunoyama, T. Akita and T. Tsukuda, *J. Phys. Chem. C*, 2009, **113**, 13457.
40. K. Guillois, L. Burel, A. Tuel and V. Caps, *Appl. Catal. A*, 2012, **415-416**, 1.



Calcining mechanical mixtures of TiO₂ and AuPPh₃Cl generates Au/TiO₂ nanocomposites with strong Au-TiO₂ interaction and high solar light activity.